Molecular Therapy
Nucleic Acids
Original Article

LINC00472 Acts as a Tumor Suppressor in NSCLC through KLLN-Mediated p53-Signaling Pathway via MicroRNA-149-3p and MicroRNA-4270

Aimei Zou,[2,4] Xingli Liu,[2,4] Zongjiong Mai,[3,4] Junke Zhang,[2] Zhuohuan Liu,[2] Qilu Huang,[1] Aibing Wu,[1] and Chenyu Zhou[2]

[1]Department of Oncology, Affiliated Hospital of Guangdong Medical University, Zhanjiang 524001, P.R. China; [2]Department of Oncology, Shunde Hospital, Southern Medical University (The First People's Hospital of Shunde), Foshan 528308, P.R. China; [3]Area 7 of Tumor Chemotherapy Department, Central Hospital of Guangdong Nongken, Zhanjiang 524001, P.R. China

Long non-coding RNAs and microRNAs (miRNAs) have been reported to participate in the progression of non-small-cell lung cancer (NSCLC). Long intergenic non-protein-coding RNA 472 (LINC00472), miR-149-3p, and miR-4270 were found to be involved in tumor activities, suggesting potential roles in NSCLC. Thus, this study aimed to examine the ability of LINC00472 to influence the progression of NSCLC with the involvement of miR-149-3p and miR-4270. Initially, differentially expressed long non-coding RNAs (lncRNAs), downstream regulatory miRNAs, and genes related to NSCLC were identified. Next, the interaction among LINC00472, miR-149-3p and miR-4270, and KLLN and the p53-signaling pathway was determined. The effect of LINC00472 on the expression of E-cadherin, N-cadherin, and Vimentin was examined through gain-of-function and loss-of-function experiments. Lastly, the effects of LINC00472 on NSCLC tumor growth were assessed *in vivo*. LINC00472 and KLLN were found to exhibit low levels, while miR-149-3p and miR-4270 were highly expressed in NSCLC. In addition, the overexpression of LINC00472 was observed to upregulate KLLN and activate the p53-signaling pathway, which ultimately inhibited the invasion, migration, and EMT of NSCLC cells via miR-149-3p and miR-4270, corresponding to decreased N-cadherin and Vimentin and increased E-cadherin. The overexpression of LINC00472 exerted an inhibitory effect on tumor growth *in vivo*. Taken together, the key evidence suggests that the overexpression of LINC00472 can downregulate miR-149-3p and miR-4270 to upregulate KLLN and activate the p53-signaling pathway, thus inhibiting the development of NSCLC. This study highlights the potential of LINC00472 as a promising therapeutic target for NSCLC treatment.

INTRODUCTION

As the foremost form of lung cancer, non-small-cell lung cancer (NSCLC) is the leading cause of death among men and women worldwide, which accounts for about 80% to 85% of all patients with lung cancer.[1,2] The epithelial-mesenchymal transition (EMT) is a pivotal event in epithelial-derived cancers during tumor invasion and metastasis, which was also found to participate in the progress of NSCLC.[3] The EMT is characterized by the altered expression of epithelial and mesenchymal markers, in addition to morphological changes.[4] At present, surgical resection represents the most common treatment as well as the gold standard for NSCLC treatment; however, the prognosis for patients with advanced NSCLC remains poor, owing largely to post-surgical recurrence rates, which chiefly depend on the final pathological stage.[5] The finer details associated with the metastatic mechanism of NSCLC are yet to be fully understood, highlighting the need for better prognostic markers for NSCLC. Accumulating evidence has illustrated that long non-coding RNAs (lncRNAs) and microRNAs (miRNAs) play a role in the development of NSCLC.[6–8]

lncRNAs represent a class of RNAs that are over 200 nt with limited or no protein-coding capacity, which have been implicated in a large variety of biological processes, such as transcriptional regulation, cell growth, and tumorigenesis.[9,10] It was demonstrated that the expression of long intergenic non-protein-coding RNA 472 (LINC00472) can be utilized as a marker of breast cancer, with high expression levels of LINC00472 reported to be indicative of better disease outcome.[11] A microarray-based gene expression analysis was performed during the current study, which predicted that LINC00472 was downregulated and miR-149-3p and miR-4270 were upregulated in NSCLC.

miR-149-3p has been found to promote cancer proliferation and motility via the coordinated suppression of tumor suppressor

Received 25 February 2019; accepted 8 June 2019;
https://doi.org/10.1016/j.omtn.2019.06.003.

[4]These authors contributed equally to this work.

Correspondence: Aibing Wu, Department of Oncology, Affiliated Hospital of Guangdong Medical University, No. 57, Renmin Avenue South, Zhanjiang 524001, Guangdong Province, P.R. China.
E-mail: wab80106@163.com
Correspondence: Chengyu Zhou, Department of Oncology, Shunde Hospital, Southern Medical University (The First People's Hospital of Shunde), No. 1, Jiazi Road, Foshan 528308, Guangdong Province, P.R. China.
E-mail: zhouchengyu1966@21cn.com

A

Name	logFC	AveExpr	t	P.Value	adj.P.Val	B
LINC00472	-2.395060009	8.985061996	-18.85023594	6.83E-38	2.33E-35	75.73888978
LINC00312	-2.353257165	7.509927035	-15.56313599	1.02E-30	8.65E-29	59.32079839
LINC01123	1.509889252	9.296575329	13.31249707	1.69E-25	6.42E-24	47.36041805
LINC01106	1.210564085	7.17551676	11.07989543	3.77E-20	6.57E-19	35.11347335

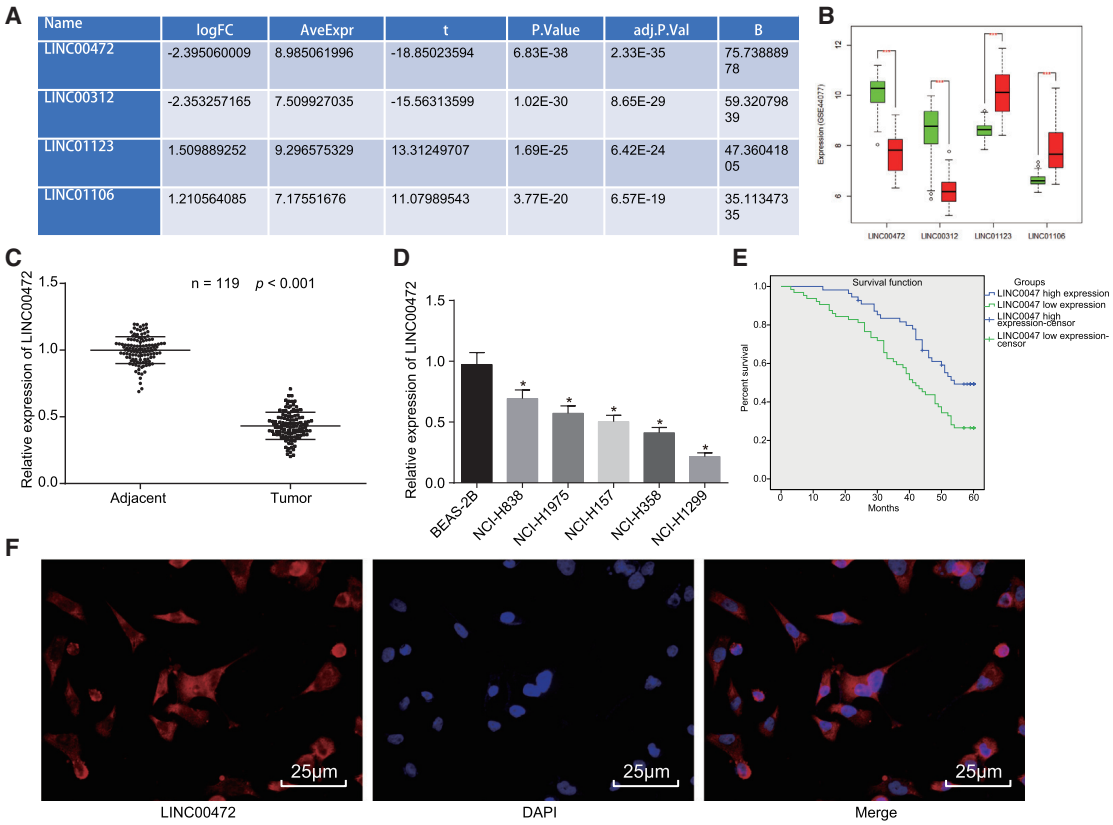

Figure 1. LINC00472 Is Lowly Expressed in NSCLC Cells and Mainly Expressed in the Cytoplasm and Nucleus

(A) The fold changes of differentially expressed LINC00472 and three other lncRNAs in GEO: GSE44077. (B) The expressions of four lncRNAs in the NSCLC-related microarray data, GEO: GSE44077. The abscissa represents the name of the lncRNA, while the ordinate is representative of the lncRNA expression in the microarray data; the green box diagram represents the normal sample, and the red box diagram represents the tumor sample. *$p < 0.005$, ***$p < 0.0001$. (C) The expression of LINC00472 in 119 cases of human NSCLC tissues and adjacent normal tissues detected by qRT-PCR, normalized by GAPDH. *$p < 0.05$ versus the adjacent normal tissues. (D) The relative expression of LINC00472 in 5 NSCLC cell lines and human normal lung epithelial cell line (BEAS-2B) detected by qRT-PCR, normalized by GAPDH. *$p < 0.05$ versus BEAS-2B cells. (E) Kaplan-Meier curves demonstrating the correlation between LINC00472 and disease prognosis in NSCLC patients. (F) Localization of the expression of LINC00472 in NCI-H1299 cells as detected by RNA-FISH (original magnification, ×400; scale bar, 25 μm). The representative measurement data were expressed as mean ± SD. Comparisons between NSCLC tissues and adjacent normal tissues were analyzed by paired t test. Comparisons among multiple groups were analyzed by one-way ANOVA. The experiment was repeated three times. LINC00472, long intergenic non-protein-coding RNA 472; NSCLC, non-small-cell lung cancer; RNA-FISH, RNA-fluorescence *in situ* hybridization.

Disabled-2 Interacting Protein in the stromal and tumor cells.[12] The existing literature has suggested that miR-4270 is highly expressed in highly metastatic gastric cancer cells, highlighting its potential as a tumor contributor in gastric cancer.[13] Moreover, the microarray-based gene expression analysis also revealed that miR-149-3p and miR-4270 could directly bind to killin (KLLN). Data obtained revealed that KLLN could stimulate the expression of p53 and p73 in the form of transcription and, thus, inhibit tumor cell growth and enhance cell apoptosis.[14] A previous study has asserted that the p53-signaling pathway is downregulated in lung cancer tissues *in vitro*, highlighting the role of the p53-signaling pathway in lung cancer cell activities.[15]

Hence, the current study aimed to investigate the mechanism by which LINC00472, miR-149-3p, miR-4270, KLLN, and the p53-signaling pathway regulate the EMT and invasion as well as the metastasis of NSCLC cells.

RESULTS

Low Expression Level of LINC00472 Is Observed in NSCLC

The GEO database was explored to retrieve the NSCLC-related microarray data. Differential expression analysis of lncRNAs in NSCLC samples and normal control samples in the microarray data was performed. Finally, 1,029 significantly differentially expressed lncRNAs were obtained from the microarray data. Among the differentially expressed lncRNAs, 4 lncRNAs exhibited significant differences. Among these 4 lncRNAs, we identified that LINC00472 was significantly downregulated in NSCLC and its downregulation was the most significant among the four lncRNAs (Figures 1A and 1B).

To verify the predicted results of the microarray-based gene expression analysis, the expression of LINC00472 in 119 cases of human NSCLC tissues and adjacent normal tissues was detected by qRT-PCR (Figure 1C), the results of which demonstrated that the expression of LINC00472 was markedly downregulated in NSCLC tissues when compared to adjacent normal tissues ($p < 0.05$). qRT-PCR was adopted to detect the relative expression of LINC00472 in NSCLC cell lines (NCI-H838, NCI-H1975, NCI-H157, NCI-H358, and NCI-H1299) and human normal lung epithelial cell line (BEAS-2B) (Figure 1D). The results revealed that, compared with BEAS-2B cells, the expression of LINC00472 in the aforementioned five human NSCLC cell lines was considerably downregulated, with the decline more pronounced in NCI-H1299 cells ($p < 0.05$).

The application of a Kaplan-Meier curve was used to analyze the association between LINC00472 and the disease prognosis in NSCLC patients (Figure 1E). The mean value of LINC00472 expression was set as the cutoff point, based on which the patients were segregated into the high-expression group (≥ 0.432) and low-expression group (<0.432). The results obtained revealed that the low expression of LINC00472 was associated with poor prognosis among NSCLC patients. The subcellular localization of LINC00472 in NCI-H1299 cells was detected by RNA-fluorescence *in situ* hybridization (FISH) assay (Figure 1F), the results of which revealed that the expression of LINC00472 was predominantly in the cytoplasm and nucleus of the NCI-H1299 cells. The aforementioned results revealed that LINC00472 was lowly expressed in the NSCLC cells and mainly located in the cytoplasm and nucleus of the NCI-H1299 cell.

Overexpression of LINC00472 Inhibits the Proliferation, Migration, Invasion, and EMT of NCI-H1299 Cells

Microarray-based gene expression analysis revealed that LINC00472 was lowly expressed in NSCLC, which led us to investigate the effects associated with the overexpression of LINC00472 on the biological properties of NSCLC NCI-H1299 cells. The plasmid transfection efficiency in the overexpression (oe)-LINC00472 group was detected by qRT-PCR (Figure 2A). The results obtained suggested that the expression of LINC00472 in the oe-LINC00472 group was significantly higher than that in the oe-negative control (NC) group ($p < 0.05$), and the transfection efficiency met the requirements for further experiments. Western blot analysis was adopted to determine the expressions of EMT-related epithelial marker (E-cadherin) and interstitial markers (N-cadherin and Vimentin) (Figure 2B). The results demonstrated that, compared with the oe-NC group, the expression of E-cadherin was significantly increased, while the expressions of N-cadherin and Vimentin were significantly decreased in the oe-LINC00472 group ($p < 0.05$).

The 5-ethynyl-2′-deoxyuridine (EdU) and Transwell assays were employed to evaluate the cell proliferation, migration, and invasion (Figures 2C and 2D), which displayed that the cell proliferation, migration, and invasion were significantly reduced in the oe-LINC00472 group compared with the oe-NC group (all $p < 0.05$). The aforementioned results suggested that upregulated LINC00472 could suppress the proliferative, migration, invasion, and EMT abilities of the NSCLC cells.

Knockdown of LINC00472 Promotes the Proliferation, Migration, Invasion, and EMT of NCI-H1299 Cells

To further elucidate the role by which LINC00472 influences the NCI-H1299 cell proliferation, migration, invasion, and EMT, NCI-H1299 cells were transfected with short hairpin (sh)-LINC00472, with sh-NC as the control. Initially, the efficiency of plasmid transfection in the sh-LINC00472 group was evaluated by the qRT-PCR method (Figure 3A). The results demonstrated that the expression of LINC00472 in the sh-LINC00472 group was markedly lower than that in the sh-NC group ($p < 0.05$), indicating the transfection efficiency met the requirement for further experiments.

Next, the quantification of EMT-related markers was determined by western blot analysis (Figure 3B), which revealed a marked decline in the expression of E-cadherin in the sh-LINC00472 group, while remarkably stimulated expression levels of N-cadherin and Vimentin were detected in comparison to the findings in the sh-NC group (all $p < 0.05$). Additionally, cell proliferation, migration, and invasion were detected by EdU and Transwell assays, respectively (Figures 3C and 3D). The findings revealed that cell proliferation, migration, and invasion in the sh-LINC00472 group were significantly elevated relative to those in the sh-NC group (all $p < 0.05$). Taken together, the aforementioned results suggested that LINC00472 silencing could contribute to the potentiated proliferation, migration, invasion, and EMT of NCI-H1299 cells.

Overexpression of LINC00472 Upregulates KLLN through Inhibiting the miR-149-3p and miR-4270 Expressions in NCI-H1299 Cells

To further obtain the downstream regulatory mechanism of LINC00472, the RNA22 database was explored to predict the potential downstream regulatory miRNAs of LINC00472. At the same time, a miRNA expression microarray dataset, GEO: GSE53882, of NSCLC was obtained. A differential expression analysis of GEO: GSE53882 revealed a significant upregulation in the expression of 104 miRNAs in NSCLC samples. An intersection of the two miRNA datasets (Figure 4A) indicated that a total of 39 miRNAs were intersected, which confirmed that these 39 miRNAs were highly likely to function as downstream regulatory miRNAs of LINC00472 in NSCLC.

Among the 39 miRNAs, miR-4270 exhibited a notably high expression pattern in NSCLC (Table S1). The prediction of the downstream target genes of miRNAs demonstrated that both miR-149-3p and miR-4270 were upregulated in NSCLC and were capable of regulating the expression of KLLN. Thus, we predicted that LINC00472 was likely to regulate both miR-149-3p and miR-4270, which further modulated the expression of their common target gene KLLN and affected the development of NSCLC. The biological prediction website (https://cm.jefferson.edu/rna22/Interactive/) was employed to determine the existence of binding sites between LINC00472 and miR-149-3p as well as miR-4270. The biological prediction website

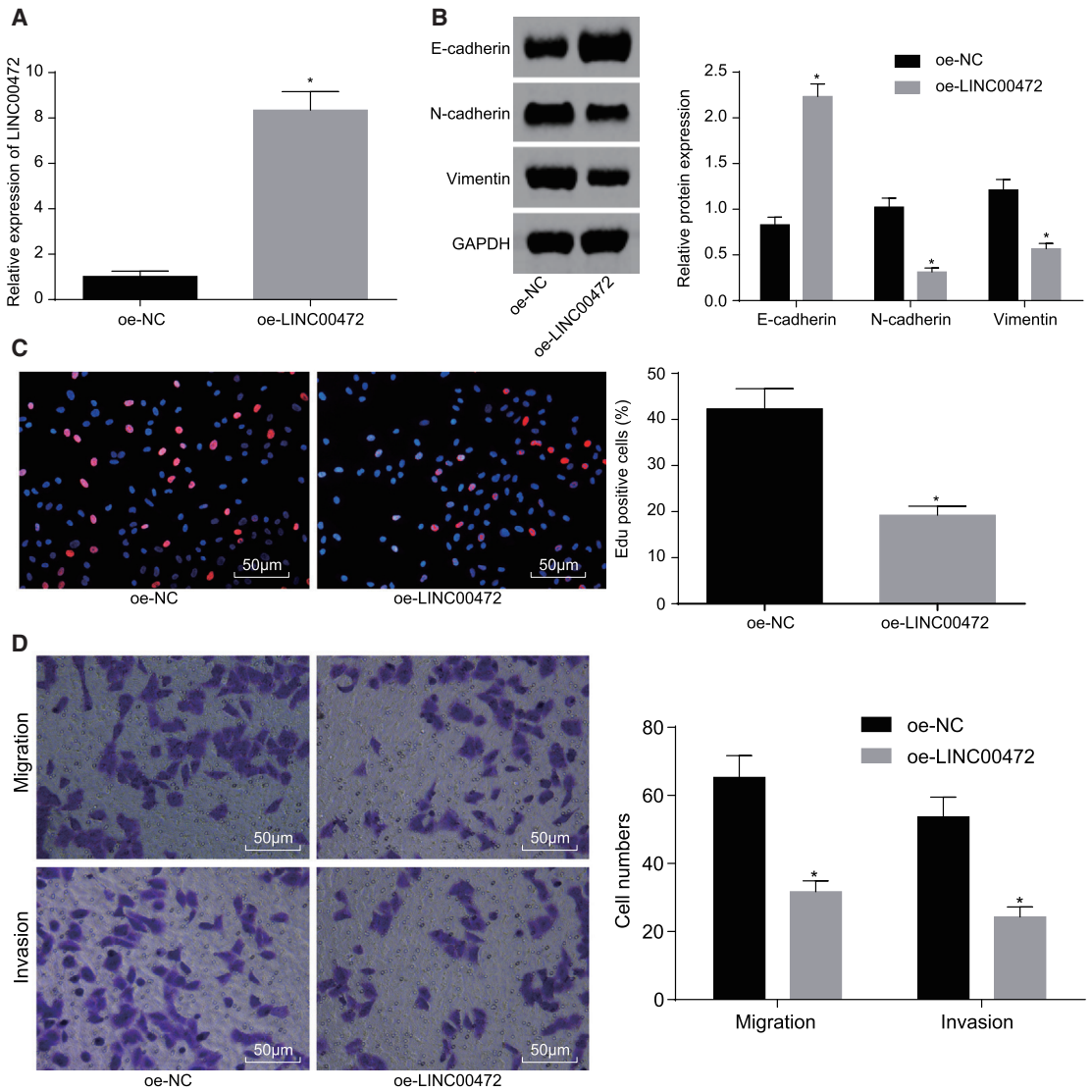

Figure 2. Overexpression of LINC00472 Represses the Proliferation, Migration, Invasion, and EMT of NCI-H1299 Cells

NCI-H1299 cells were transfected with oe-LINC00472 or oe-NC. (A) The transfection efficiency of the overexpression of LINC00472 detected by qRT-PCR, normalized by GAPDH. (B) The expressions of EMT-related markers detected by western blot analysis. (C) Cell proliferation of each group detected by EdU assay (the original magnification is ×200). (D) Cell migration and invasion in each group detected by Transwell assay (the original magnification is ×200). *$p < 0.05$ versus the oe-NC group. The representative measurement data were expressed as mean ± SD. Comparisons between two groups were analyzed by unpaired t test. Comparisons among multiple groups were analyzed by one-way ANOVA. The experiment was repeated three times. LINC00472, long intergenic non-protein-coding RNA 472; NSCLC, non-small-cell lung cancer; EMT, epithelial-mesenchymal transition; GAPDH, glyceraldehyde-3-phosphate dehydrogenase.

(http://www.mirbase.org/) was explored to determine whether both miR-149-3p and miR-4270 have binding sites with KLLN (Figure 4B).

The expressions of miR-149-3p and miR-4270 in the tissues and cells were measured by qRT-PCR (Figure 4C), the results of which showed that miR-149-3p and miR-4270 were upregulated in NSCLC cells and tissues ($p < 0.05$). Besides, miR-149-3p and miR-4270 were both found to be negatively correlated with the expression of LINC00472 (Figure 4D). Subsequently, we confirmed that LINC00472 negatively regulated the expression of miR-149-3p and miR-4270 and positively regulated KLLN (Figure 4E). Furthermore, miR-149-3p and miR-4270 in turn negatively regulated the expression of KLLN (Figure 4F).

A dual-luciferase reporter gene assay was adopted to determine the fluorescence intensity of the NC mimic, miR-149-3p mimic, and miR-4270 mimic respectively co-transfected with wild-type (WT)-LINC00472, mutant-type (mut)-LINC00472, WT-KLLN, and mut-KLLN (Figure 4G). The results obtained suggested that, compared

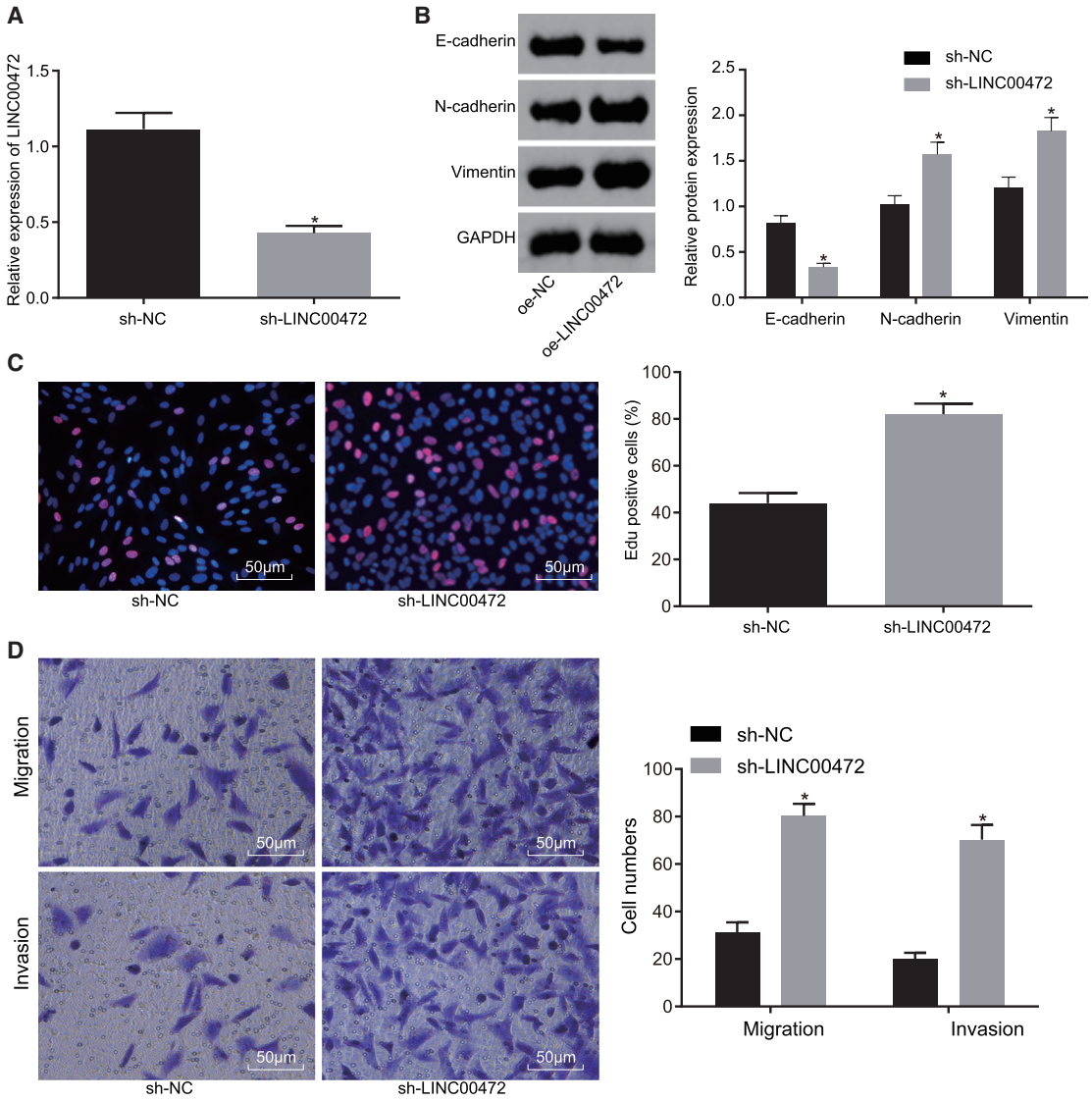

Figure 3. Silencing of LINC00472 Facilitates the Proliferation, Migration, Invasion, and EMT of NCI-H1299 Cells

NCI-H1299 cells were transfected with sh-LINC00472 or sh-NC. (A) The transfection efficiency of the silencing of LINC00472 detected by qRT-PCR, normalized by GAPDH. (B) The expressions of EMT-related markers detected by western blot analysis, normalized by GAPDH. (C) Cell proliferation of each group detected by EdU assay (the original magnification is ×200). (D) Cell migration and invasion in each group detected by Transwell assay (the original magnification is ×200). *$p < 0.05$ versus the sh-NC group. The representative measurement data were expressed as mean ± SD. Comparisons between two groups were analyzed by unpaired t test. Comparisons among multiple groups were analyzed by one-way ANOVA. The experiment was repeated three times. LINC00472, long intergenic non-protein-coding RNA 472; NSCLC, non-small-cell lung cancer; EMT, epithelial-mesenchymal transition; GAPDH, glyceraldehyde-3-phosphate dehydrogenase.

with the NC mimic group, the fluorescence intensity was significantly decreased after miR-149-3p mimic and miR-4270 mimic were respectively co-transfected with WT-LINC00472 and WT-KLLN ($p < 0.05$), while no significant difference was detected regarding the fluorescence intensity after miR-149-3p mimic and miR-4270 mimic were respectively co-transfected with mut-LINC00472 and mut-KLLN ($p > 0.05$). The RNA-binding protein immunoprecipitation (RIP) assay results revealed that miR-149-3p and miR-4270 could bind to LINC00472 or KLLN (Figure 4H).

The qRT-PCR and western blot analysis were employed to detect the expression of KLLN in the NC mimic group, miR-149-3p mimic group, miR-149-3p mimic + oe-NC group, and miR-149-3p mimic + oe-LINC00472 group; and the NC mimic group, miR-4270 mimic group, miR-4270 mimic + oe-NC group, and miR-4270 mimic + oe-LINC00472 group (Figure 4I). The results revealed that, compared with the NC mimic group, the expression of KLLN was remarkably decreased in the miR-149-3p mimic group and the miR-4270 mimic group (both $p < 0.05$). Compared with the miR-149-3p

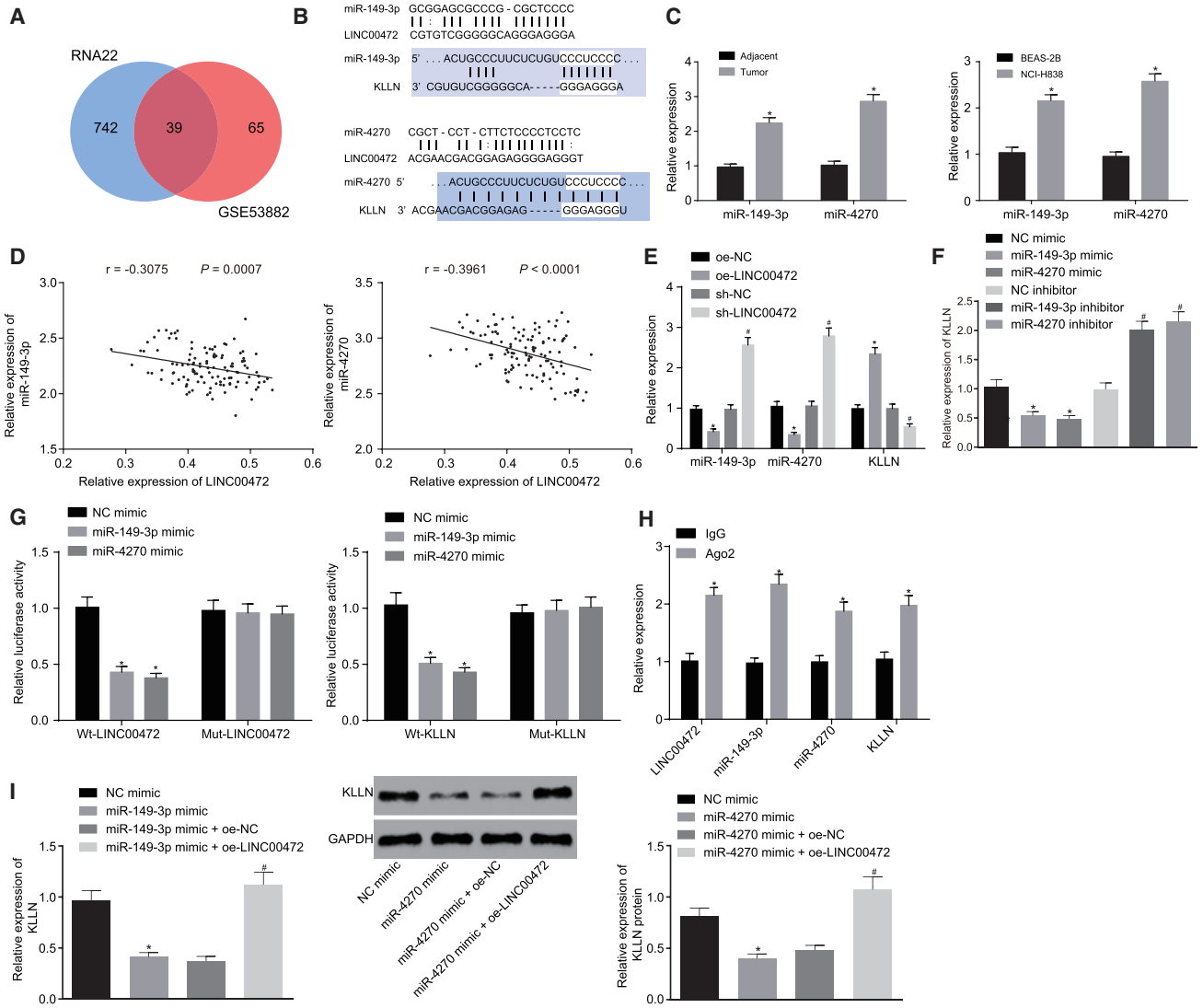

Figure 4. Overexpression of LINC00472 Upregulates the KLLN Expression through Modulating the miR-149-3p and miR-4270 Expressions in NCI-H1299 Cells

NCI-H1299 cells were transfected with miR-149-3p mimic or miR-4270 mimic alone or with oe-LINC00472. (A) Prediction of LINC00472 downstream regulatory miRNAs. The left circle indicates prediction results of the RNA22 database, the right circle indicates the GEO: GSE53882 chip analysis results, and the overlapping part indicates the intersection of the two sets of data. (B) Binding sites predicted by the RNA22 database of miR-149-3p and miR-4270, respectively, with LINC00472 and KLLN, and binding sites predicted by TargetScan of miR-149-3p and miR-4270, respectively, with LINC00472 and KLLN. (C) The qRT-PCR demonstrating the expression of miR-149-3p and miR-4270 in tissues and cells, normalized by U6. *p < 0.05 versus the adjacent normal tissues or the BEAS-2B cells. (D) Correlation analysis of miR-149-3p and miR-4270, respectively, with LINC00472. (E) The qRT-PCR demonstrating the effect of overexpression or silencing of LINC00472 on miR-149-3p, miR-4270, and KLLN, normalized by U6 or GAPDH. *p < 0.05 versus oe-NC group, #p < 0.05 versus the sh-NC group. (F) The qRT-PCR demonstrating the effect of overexpression or silencing of miR-149-3p and miR-4270, respectively, on the expression of KLLN, normalized by U6 or GAPDH. *p < 0.05 versus the NC mimic group, #p < 0.05 versus the NC inhibitor group. (G) The dual-luciferase reporter assay showing the fluorescence intensity of NC mimic, miR-149-3p mimic, and miR-4270 mimic separately co-transfected with WT-LINC00472, mut-LINC00472, WT-KLLN, and mut-KLLN. *p < 0.05 versus NC mimic group. (H) RIP assay showing miR-149-3p and miR-4270, respectively, binding to LINC00472 or KLLN. *p < 0.05 versus the anti-IgG group. (I) The qRT-PCR and western blot analysis showing the expression of KLLN. *p < 0.05 versus the NC mimic group, #p < 0.05 versus the miR-149-3p mimic + oe-NC group or the miR-4270 mimic + oe-NC group. The representative measurement data were expressed as mean ± SD. Comparisons between the NSCLC tissues and adjacent normal tissues were analyzed by paired t test, and other comparisons between two groups were analyzed by unpaired t test. Comparisons among multiple groups were analyzed by one-way ANOVA. Pearson correlation analysis was performed between miR-149-3p, miR-4270, respectively, and LINC00472. The experiment was repeated three times. LINC00472, long intergenic non-protein-coding RNA 472; NSCLC, non-small-cell lung cancer; miR-149-3p, microRNA-149-3p; miR-4270, microRNA-4270; RIP, RNA-binding protein immunoprecipitation.

mimic + oe-NC group or the miR-4270 mimic + oe-NC group, the expression of KLLN was significantly increased in the miR-149-3p mimic + oe-LINC00472 group or miR-4270 mimic + oe-LINC00472 group (both $p < 0.05$). Taken together, the above results provide evidence suggesting that overexpressed LINC00472 could upregulate the expression of KLLN by inhibiting the expression of miR-149-3p and miR-4270.

Overexpression of LINC00472 Reduces the EMT, Migration, and Invasion of NCI-H1299 Cells through Sponging miR-149-3p and miR-4270

To evaluate the combined effects of LINC00472 and miR-149-3p or miR-4270, the mRNA and protein expressions of EMT-associated epithelial marker (E-cadherin) and interstitial markers (N-cadherin and Vimentin) in NCI-H1299 cells were evaluated accordingly by qRT-PCR and western blot analysis (Figure 5A). The results revealed that, compared to the NC mimic group, the expression of E-cadherin in the miR-149-3p mimic or miR-4270 mimic groups notably diminished (both $p < 0.05$), while the expressions of N-cadherin and Vimentin were markedly elevated (both $p < 0.05$). Compared to the miR-149-3p mimic + oe-NC group or the miR-4270 mimic + oe-NC group, the miR-149-3p mimic + oe-LINC00472 group or the miR-4270 mimic + oe-LINC00472 group distinctly promoted expression levels of E-cadherin (both $p < 0.05$), while significantly diminished expressions of N-cadherin and Vimentin were identified (both $p < 0.05$).

Similarly, cell proliferation, migration, and invasion assessed by EdU and Transwell assays (Figures 5B–5D) revealed that, compared with the NC mimic group, miR-149-3p mimic or miR-4270 mimic treatment led to enhanced cell proliferation, migration, and invasion (all $p < 0.05$). However, the addition of oe-LINC00472 was found to be capable of rescuing miR-149-3p mimic- or miR-4270 mimic-induced stimulation of proliferation, invasion, and migration relative to that of oe-NC (all $p < 0.05$). These results suggest that the proliferation, invasion, migration, and EMT of NCI-H1299 cells could be hindered by miR-149-3p- or miR-4270-dependent LINC00472 overexpression.

Overexpression of LINC00472 Activates the p53-Signaling Pathway and Inhibits the EMT, Migration, and Invasion of NCI-H1299 Cells through Upregulating the Expression of KLLN

A gene interaction network map was constructed based on the correlation analysis between KLLN and the known genes related to NSCLC retrieved from the DisGeNET database (Figure 6A). Evidence was obtained suggesting that only the KLLN gene interacted with known genes related to NSCLC, among which the direct regulation of TP53 by KLLN has been previously validated.[16] Meanwhile, the TP53 gene was at the core of the p53-signaling pathway (map: 04115), and the TP53 gene and the p53-signaling pathway were identified to play a role in the progression of various neoplastic diseases.[17–20] The immunohistochemistry results demonstrated (Figure 6B) that the expression of KLLN was significantly lower in NSCLC tissues than in adjacent normal tissues ($p < 0.05$). Besides, the qRT-PCR results suggested (Figure 6C) that, relative to the normal lung epithelial cell line (BEAS-2B), the expression of KLLN was also remarkably decreased in the NSCLC cell line NCI-H1299 ($p < 0.05$). We detected that LINC00472 was positively correlated with KLLN expression, based on our correlation analysis (Figure 6D).

Next, NCI-H1299 cells were co-transfected with oe-LINC00472 and sh-NC or sh-KLLN, and the transfection efficiency was detected by qRT-PCR (Figure 6E). Compared with the oe-NC + sh-NC group, the transfection efficiencies of the oe-LINC00472 + sh-NC group and the oe-LINC00472 + sh-KLLN group met the requirements for further experiments ($p < 0.05$). The qRT-PCR and western blot analysis were employed to evaluate the expression of p53, p21, as well as the epithelial markers (E-cadherin) and interstitial markers (N-cadherin and Vimentin) related to the EMT (Figure 6F). Compared with the oe-NC + sh-NC group, the expressions of p53, p21, and E-cadherin in the oe-LINC00472 + sh-NC group were significantly increased, while those of N-cadherin and Vimentin were notably decreased (all $p < 0.05$); the expressions of p53, p21, and E-cadherin in the oe-LINC00472 + sh-KLLN group were significantly decreased, while the expressions of N-cadherin and Vimentin were significantly increased (all $p < 0.05$).

Cell proliferation, migration, and invasion were detected by EdU and Transwell assays (Figures 6G and 6H), the results of which revealed that, compared with the oe-NC + sh-NC group, the cell proliferation, migration, and invasion were remarkably decreased in the oe-LINC00472 + sh-NC group (all $p < 0.05$), while the cell proliferation, migration, and invasion in the oe-LINC00472 + sh-KLLN group were evidently increased (all $p < 0.05$). The aforementioned results provided confirmation indicating that the overexpression of LINC00472 activates the p53-signaling pathway and further inhibits the EMT, migration, and invasion of NSCLC cells via the upregulation of KLLN expression.

Overexpression of LINC00472 Inhibits Tumor Formation and Growth of NSCLC Cells *In Vivo*

In an attempt to validate the effect associated with LINC00472 on the development of tumor xenografts *in vivo*, the nude mice were assigned to the oe-NC group and the oe-LINC00472 group. The tumor xenograft in nude mice experiment (Figure 7A) indicated that, compared with the oe-NC group, the mean volume of tumor xenografts in the oe-LINC00472 group was significantly reduced ($p < 0.05$). qRT-PCR was adopted to measure the expressions of LINC00472, miR-149-3p, and miR-4270 in tumor xenografts in the two groups (Figure 7B), the results of which demonstrated that the expression of LINC00472 was significantly increased in the oe-LINC00472 group when compared to the oe-NC group ($p < 0.05$), while the expressions of miR-149-3p and miR-4270 were significantly decreased ($p < 0.05$).

Next, the expressions of KLLN, E-cadherin, N-cadherin, Vimentin, p21, p53, and cyclin D1 in the two groups were detected by immunohistochemistry (Figure 7C), the results of which revealed that, compared with the oe-NC group, the expressions of KLLN,

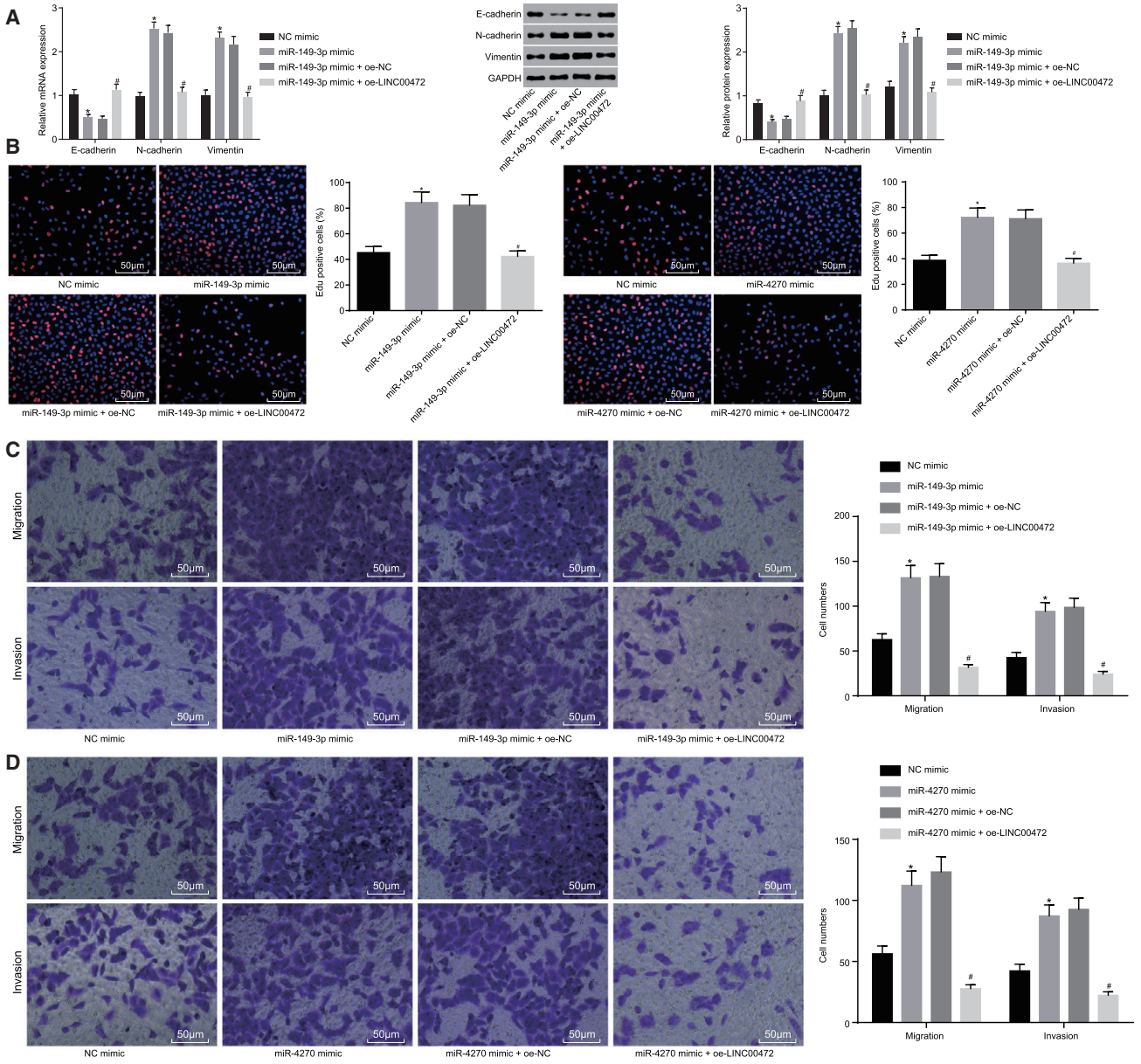

Figure 5. Overexpression of LINC00472 Inhibits the EMT, Migration, and Invasion of NCI-H1299 Cells through Inhibiting miR-149-3p and miR-4270 Expressions

NCI-H1299 cells were transfected with miR-149-3p mimic or miR-4270 mimic alone or with oe-LINC00472. (A) The qRT-PCR and western blot analysis showing the expressions of EMT-related epithelial marker (E-cadherin) and interstitial markers (N-cadherin and Vimentin), normalized by GAPDH. (B) EdU assay showing the proliferation of cells in each group (the original magnification is ×200). (C and D) Transwell assay showing the migration and invasion in each group (the original magnification is ×200). *$p < 0.05$ versus the NC mimic group, #$p < 0.05$ versus the miR-149-3p mimic + oe-NC group or the miR-4270 mimic + oe-NC group. The representative measurement data were expressed as mean ± SD. Comparisons between two groups were analyzed by unpaired t test. The experiment was repeated three times. LINC00472, long intergenic non-protein-coding RNA 472; NSCLC, non-small-cell lung cancer; miR-149-3p, microRNA-149-3p; miR-4270, microRNA-4270; EMT, epithelial-mesenchymal transition.

E-cadherin, p53, and p21 were significantly upregulated in the oe-LINC00472 group ($p < 0.05$), while those of N-cadherin, Vimentin, and cyclin D1 were remarkably decreased ($p < 0.05$). The above results provided evidence suggesting that high LINC00472 expression inhibits the development of NSCLC cells *in vivo*.

DISCUSSION

NSCLC remains one of the foremost malignancies afflicting the lungs, and it is characterized by rapid growth and aggressive features during its progression, leading to a large number of deaths on an annual basis worldwide.[21] Recent reports have indicated that LINC00472 assumes

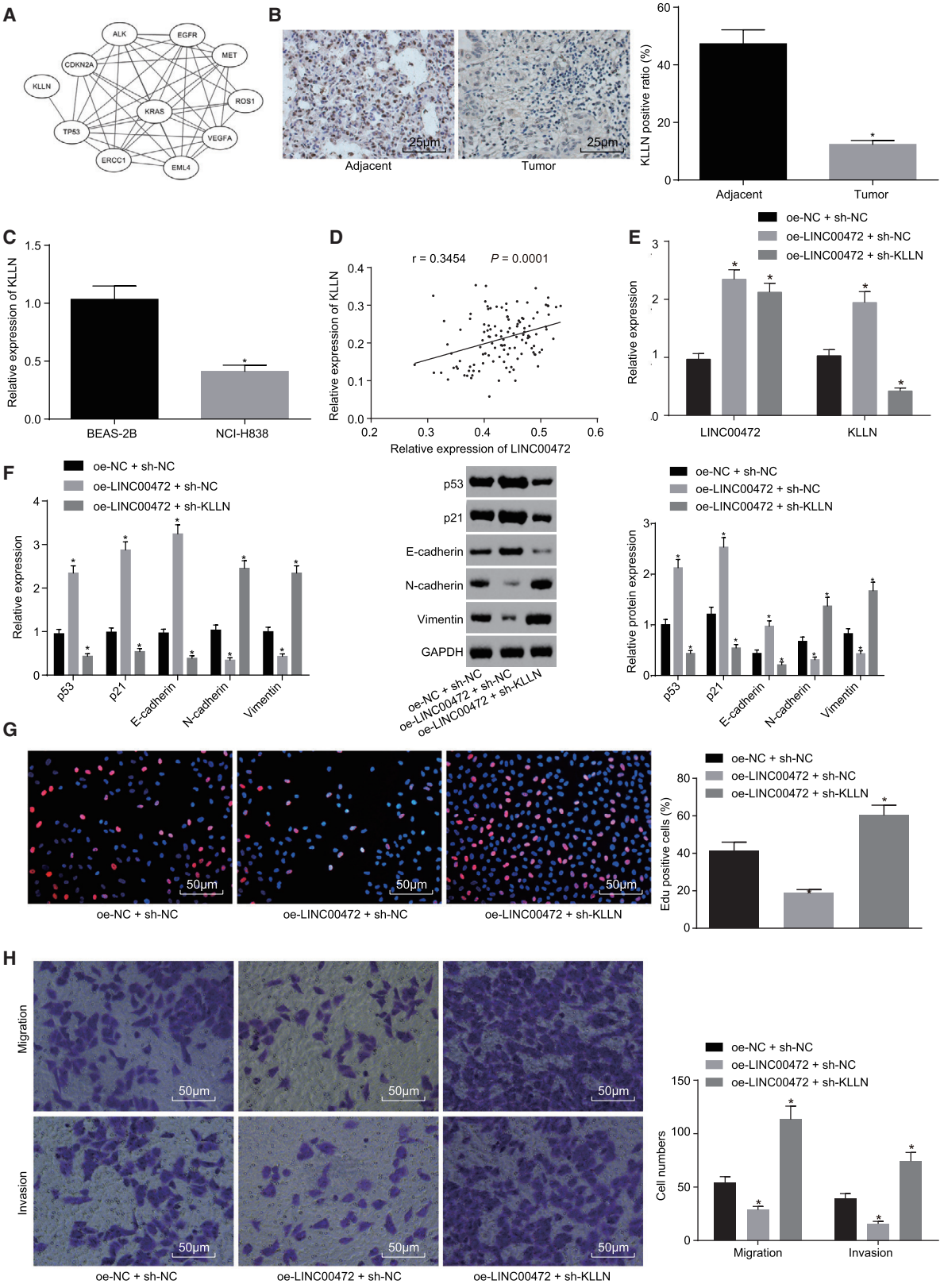

(legend on next page)

a tumor-suppressive role in various types of cancers, including gastric cancer, epithelial ovarian cancer, and colorectal cancer.[22–24] However, the role of LINC00472 functioning in NSCLC has remained largely unknown. The results obtained during our study suggested that the overexpression of LINC00472 upregulated the expression of KLLN and further activated the p53-signaling pathway, resulting in the suppression of migration, invasion, and the EMT of NSCLC cells by inhibiting the expressions of miR-149-3p and miR-4270.

Our initial observations revealed that LINC00472 and KLLN were lowly expressed while miR-149-3p and miR-4270 were highly expressed in NSCLC. Interestingly, consistent with our findings, a previous study using a lncRNA-mediated competing endogenous RNA (ceRNA) network investigated potential lncRNA biomarkers in lung adenocarcinoma, and it concluded that LINC00472 was downregulated in lung adenocarcinoma tissues.[25] Several lncRNAs have been highlighted due to their tumor-suppressive abilities in NSCLC. For example, the expression of lncRNA-p21 expression has been demonstrated to be lower in NSCLC tissues when compared to paired normal tissues, suggesting that increased levels of lncRNA-p21 are associated with longer overall and disease-free survival of NSCLC patients.[26] The expression level of lncRNA HMlincRNA717 was also found decreased in NSCLC tissues, and HMlincRNA717 was suggested as the therapeutic target in the treatment of patients with NSCLC.[27] The existing literature has presented evidence illustrating that KLLN is downregulated in breast cancer, suggesting that it plays a tumor suppressor role in breast cancer.[16] A study analyzed miR-149-3p expression in data obtained from The Cancer Genome Atlas (TCGA) consortium, and it found that miR-149-3p was upregulated in human malignancies, including lung cancer.[12] Furthermore, miR-4270 has been found to be upregulated in immune thrombocytopenic purpura and sepsis-induced acute kidney injury, in addition to displaying upregulated levels in gastric cancer and breast cancer patients.[13,28–30]

Next, it has been shown that LINC00472 competitively bound to both miR-149-3p and miR-4270, which could target KLLN to regulate the p53-signaling pathway in NSCLC. LINC00472 as a tumor suppressor in colorectal cancer cells has been proven to bind to miR-196a and play a crucial role in the ceRNA regulatory network.[24] KLLN, as a target gene of miR-224, functions as proto-oncogene or anti-oncogene in various types of cancer cells.[31] Gene correlation analysis demonstrated the existence of a strong correlation between KLLN and the TP53 gene, which is involved in the progression of tumors associated with the p53-signaling pathway.[17,19] Wang et al.[14] concluded that KLLN could upregulate the expression of TP53 and TP73, which ultimately acts to promote cell apoptosis in prostate cancer. Besides, the overexpression of lncRNA MEG3 inhibits the proliferation and metastasis of gastric cancer by activating the p53-signaling pathway.[32]

In the subsequent assays, we found that over-regulation of LINC00472 downregulated miR-149-3p and miR-4270 to inhibit the invasion, migration, and EMT of NSCLC cells, corresponding to the high expression of E-cadherin and low expressions of N-cadherin and Vimentin. Consistently, it has been confirmed that overexpressed LINC00472 is capable of suppressing the proliferation while stimulating apoptosis through regulating miR-24-3p in lung adenocarcinoma cells, which may be a potential biomarker and therapeutic target for lung adenocarcinoma.[33] Another lncRNA, LINC01186, has been suggested to inhibit the migration and invasion of lung cancer cells by mediating the transforming growth factor β (TGF-β)-signaling pathway.[34] In the current study, LINC00472 was demonstrated to inhibit NSCLC cell EMT, migration, and invasion by upregulating the expression of KLLN. LINC01133 has been indicated to suppress colorectal cancer through the inhibition of tumor cell metastasis and EMT, corresponding to upregulated levels of E-cadherin and downregulated Vimentin.[35] Furthermore, based on an *in vivo* assay, evidence has been presented demonstrating that the upregulation of LINC00472 inhibited the tumor growth of NSCLC.

Based on our *in vitro* and *in vivo* experiments, we obtained data indicating that the overexpression of LINC00472 upregulates KLLN to inhibit the proliferation, invasion, and EMT of NSCLC cells through the downregulation of miR-149-3p and miR-4270 (Figure 8). We uncovered encouraging data that placed further emphasis on the value of LINC00472 as a potential novel therapeutic target for NSCLC. Nevertheless, due to the limited cases and lack of clinical value development, the effectiveness of our findings from a clinical perspective will be confirmed in the future by a large-sample, multicenter, and randomized controlled trial.

Figure 6. Overexpressed LINC00472 Activates the p53-Signaling Pathway by Upregulating the Expression of KLLN to Suppress the EMT, Migration, and Invasion of NCI-H1299 Cells

NCI-H1299 cells were co-transfected with oe-LINC00472 and sh-NC or sh-KLLN, with oe-NC or sh-NC as the control. (A) Correlation analysis of core target genes and NSCLC-related known genes. Each ellipse in the figure represents a gene, and the line between the ellipses indicates the interaction between the two genes. (B) The immunohistochemistry showing the expression of KLLN in NSCLC tissues (the original magnification is ×400). *$p < 0.05$ versus the adjacent normal tissues. (C) The qRT-PCR showing the expression of KLLN in NSCLC cells, normalized by GAPDH. *$p < 0.05$ versus the BEAS-2B cells. (D) Correlation analysis of LINC00472 and KLLN expression. (E) The qRT-PCR showing the transfection efficiency of each group. (F) The qRT-PCR and western blot analysis showing the expression of p53 and epithelial marker (E-cadherin) and interstitial markers (N-cadherin and Vimentin) related to the EMT, normalized by GAPDH. (G) The EdU assay showing cell proliferation (the original magnification is ×200). (H) The Transwell assay showing cell migration and invasion (the original magnification is ×200). *$p < 0.05$ versus the oe-NC + sh-NC group (E–H). The representative measurement data were expressed as mean ± SD. Comparisons between the NSCLC tissues and adjacent normal tissues were analyzed by paired t test, and other comparisons between two groups were analyzed by unpaired t test. Comparisons among multiple groups were analyzed by one-way ANOVA. Pearson correlation analysis was performed between LINC00472 and KLLN. The experiment was repeated three times. LINC00472, long intergenic non-protein-coding RNA 472; NSCLC, non-small-cell lung cancer; EMT, epithelial-mesenchymal transition; GAPDH, glyceraldehyde-3-phosphate dehydrogenase.

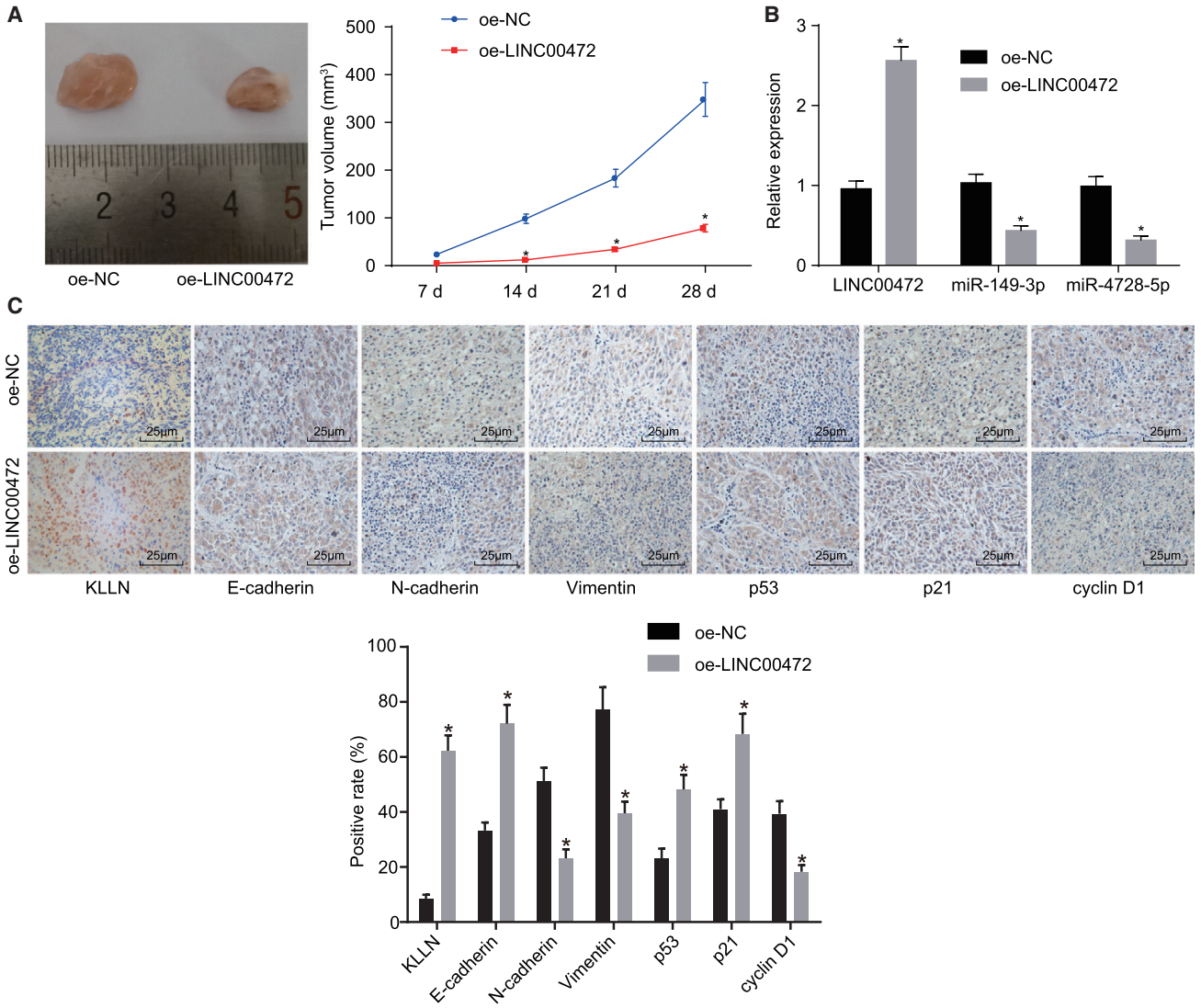

Figure 7. Overexpressed LINC00472 Suppresses Tumor Growth of NCI-H1299 Cells *In Vivo*

The nude mice were injected with NCI-H1299 cells harboring oe-LINC00472 or oe-NC. (A) The images and mean volume of the tumor xenografts in the two groups of NCI-H1299 cells with stable transfection of oe-NC and oe-LINC00472 in nude mice. (B) The qRT-PCR demonstrating the expressions of LINC00472, miR-149-3p, and miR-4270 of tumor xenografts in the two groups, normalized by U6 or GAPDH. (C) Immunohistochemistry showing the expressions of related factors in tumors of the two groups (the original magnification is × 400). *$p < 0.05$ versus the oe-NC group. The representative measurement data were expressed as mean ± SD. Comparisons between two groups were analyzed by unpaired t test. Data at different time points were compared by repeated-measurement ANOVA. LINC00472, long intergenic non-protein-coding RNA 472; miR-149-3p, microRNA-149-3p; miR-4270, microRNA-4270; NSCLC, non-small-cell lung cancer.

MATERIALS AND METHODS

Ethics Statement

All experimental protocols were performed with the approval of the ethics committee of the Affiliated Hospital of Guangdong Medical University. Informed written consent was obtained from each patient. All animal experiments were in line with the Guide for the Care and Use of Laboratory Animal by International Committees. Extensive efforts were made to ensure minimal suffering of the animals used during the study.

Microarray-Based Gene Expression Analysis

The GEO database (https://www.ncbi.nlm.nih.gov/geo/) was retrieved to obtain the microarray data of NSCLC. The R-language limma package was utilized for differential expression analysis. The expression of LINC00472 in the cells was obtained from the lncATLAS database (http://lncatlas.crg.eu/). The downstream miRNAs of LINC00472 and target genes of miRNAs were predicted by the RNA22 database (https://cm.jefferson.edu/rna22/). The known NSCLC-related disease genes were obtained from the DisGeNET

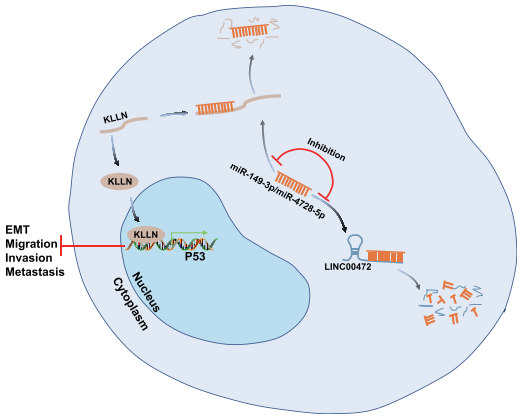

Figure 8. Schematic Representation of the Role of LINC00472 in NSCLC
Overexpression of LINC00472 upregulated the expression of KLLN and further activated the p53-signaling pathway to suppress the migration, invasion, and EMT of NSCLC cells by inhibiting miR-149-3p and miR-4270 expressions.

database (http://www.disgenet.org/), with the correlation analysis between the candidate target genes of miRNAs as well as the known disease genes performed by the STRING database (https://string-db.org/). Finally, the p53-related-signaling pathway was retrieved by the Kyoto Encyclopedia of Genes and Genomes (KEGG) metabolic pathway database (https://www.kegg.jp/kegg/pathway.html).

Sample Collection and Cell Culture

A total of 119 fresh frozen NSCLC tissue specimens as well as corresponding adjacent normal tissue specimens was collected from patients who had previously undergone a surgical procedure at the Affiliated Hospital of Guangdong Medical University between June 2017 and July 2018. All patients were followed up for 5 years, with a follow-up rate of 97.47% (116/119). Five NSCLC cell lines, NCI-H838, NCI-H1975, NCI-H157, NCI-H358, and NCI-H1299 cells, and human normal lung epithelial cell line (BEAS-2B) were purchased from the National Experimental Cell Resource Sharing Platform (http://www.cellresource.cn/). The cells were incubated in DMEM (Gibco, Carlsbad, CA, USA) complete medium containing 10% fetal bovine serum (FBS), 100 μg/mL streptomycin, and 100 U/mL penicillin in an incubator with 5% CO_2 and 95% saturated humidity at 37°C. Cell passage was performed when cell growth density reached approximately 90%. The qRT-qPCR was employed to determine the expression of LINC00472 in these five NSCLC cell lines, with the cell line exhibiting the lowest LINC00472 expression being screened out for subsequent experiments.

Cell Transfection

NSCLC cells were transfected with plasmids of oe-NC, oe-LINC00472, sh-NC, sh-LINC00472, NC inhibitor, miR-149-3p inhibitor, miR-4270 inhibitor, NC mimic, miR-149-3p mimic, miR-149-3p mimic + oe-NC, and miR-149-3p mimic + oe-LINC00472; and NC mimic, miR-4270 mimic, miR-4270 mimic + oe-NC, miR-4270 mimic + oe-LINC00472, oe-NC + sh-NC, oe-LINC00472 + sh-NC, and oe-LINC00472 + sh-KLLN. All target plasmids were purchased from Dharmacon (Lafayette, CO, USA). The cell density was adjusted according to the cell growth rate, and the cells were seeded in a 6-well plate to reach a confluence of 80%–90% on the second day of transfection. The Lipofectamine 2000 kit (Invitrogen, Carlsbad, CA, USA) was employed for cell transfection, in accordance with the protocols provided by the manufacturer. Next, 250 μL Opti-MEM medium (Gibco, Carlsbad, CA, USA) was used to dilute 4 μg target plasmid and 10 μL Lipofectamine 2000 accordingly. After thorough mixing and reservation for 5 min at room temperature, the two diluted solutions were uniformly mixed together and allowed to stand for another 20 min. The mixture of Lipofectamine 2000 as well as the plasmids was subsequently added to the wells coated with cells. After 8 h of transfection, fresh medium was replaced for an additional 48-h period of incubation for a subsequent experiment.

Table 1. Primer Sequences for qRT-PCR

Gene	Primer Sequence
LINC00472	F: 5′-GATGGCAGCTGTCTCTCTCC-3′
	R: 5′-GGGCCTCTCTGACCGTATCT-3′
KLLN	F: 5′-ATGGATCGCCCGGGGCCAG-3′
	R: 5′-TCAGTCCTTTGGCTTGCTCTTA-3′
miR-149-3p	F: 5′-TTGACGAGGGAGGGACGG-3′
	R: 5′-GCCATAAGCGAGCAGTAGCG-3′
miR-4270	F: 5′-TCAGGGAGTCAGGG-3′
	R: 5′-TGTCGTGGAGTCGGC-3′
GAPDH	F: 5′-GGGCCAAAAGGGTCATCATC-3′
	R: 5′-ATGACCTTGCCCACAGCCTT-3′
p53	F: 5′-TCAACAAGATGTTTTGCCAACTG-3′
	R: 5′-ATGTGCTGTGACTGCTTGTAGATG-3′
U6	F: 5′-CTCGCTTCGGCAGCACA-3′
	R: 5′-AACGCTTCACGAATTTGCGT-3′
E-cadherin	F: 5′-AGGCTAGAGGGTCACCGCGTC-3′
	R: 5′-GCTTTGCAGTTCCGACGCCAC-3′
N-cadherin	F: 5′-GACAATGCCCCTCAAGTGTT-3′
	R: 5′-CCATTAAGCCGAGTGATGGT-3′
Vimentin	F: 5′-GACGCCATCAACACCGAGTT-3′
	R: 5′-CTTTGTCGTTGGTTAG CTGGT-3′

F, forward; R, reverse; LINC00472, long intergenic non-protein-coding RNA 472; miR-149-3p, microRNA-149-3p; miR-4270, microRNA-4270; GAPDH, glyceraldehyde-3-phosphate dehydrogenase.

RNA Isolation and Quantitation

Total RNA was extracted using an RNeasy Mini Kit (QIAGEN, Valencia, CA, USA) and reversely transcribed into cDNA using the reverse transcription kit (RR047A, Takara Bio, Otsu, Shiga, Japan). The SYBR Premix EX Taq kit (RR420A, Takara Bio, Otsu, Shiga, Japan) was applied for sample loading, and the samples were subjected to qPCR in a real-time fluorescence qPCR (ABI7500, Applied Biosystems, Foster City, CA, USA). Three replicate wells were set for each sample. All primers (Table 1) were synthesized by Shanghai

Sangon Biological Engineering Technology & Services (Shanghai, China). The Ct value of each well was recorded, with U6 serving as the internal control for miR-149-3p and miR-4270, while glyceraldehyde-3-phosphate dehydrogenase (GAPDH) was regarded as the internal control for the other genes. The relative expression of the product was calculated based on the $2^{-\rho\rho Ct}$ method.

FISH

The subcellular localization of LINC00472 was identified through FISH assay, as per the instructions of Ribo lncRNA FISH Probe Mix (Red) (C10920, RiboBio, Guangzhou, Guangdong, China). The cell slides were placed in a 24-well culture plate, and cells were inoculated at a density of 6×10^4 cells/well, so that the cell confluence reached 60%–70%. The cells were then fixed at room temperature for 10 min with 1 mL 4% polyformaldehyde and washed accordingly. After that, the cells in each well were permeabilized at 4°C for 5 min with 1 mL pre-cooled 0.5% Triton X-100 in PBS. The cells in each well were then blocked with 200 μL pre-hybridization solution at 37°C for 30 min. After removal of the pre-hybridization solution, probe hybridization solution containing anti-LINC00472 nucleotide probe (Wuhan Genecreate Bioengineering, Wuhan, Hubei, China) was added to hybrid overnight at 37°C under dark conditions. The following steps were all conducted under conditions void of light. The cells were washed 3 times in a successive manner using washing buffer I (4 × standard saline citrate [SSC] containing 0.1% Tween-20), washing buffer II (2 × SSC), washing buffer III (1 × SSC), and 1 × PBS respectively (5 min each time). The cells were stained with DAPI staining solution diluted at a ratio of 1:800 for 10 min, washed, and sealed with nail polish. Finally, 5 different views were selected and analyzed under a fluorescence microscope (Olympus Optical, Tokyo, Japan) with images subsequently obtained.

Immunohistochemistry

The tissue sections were placed in a 60°C incubator for 1 h, dewaxed by conventional xylene, hydrated with gradient ethanol, incubated with PBS containing 0.5% Triton for 20 min at room temperature, and washed 2–3 times with PBS (5–10 min each time). After being repaired for 2 min with high-pressure antigen, the sections were boiled at 95°C for 20 min in 0.01 M citric acid buffer (pH 6.0), immersed in 3% H_2O_2 for 15 min to block the exogenous peroxidase activity, and sealed with 3% BSA at 37°C for 20–30 min. The sections were subsequently incubated with the primary antibodies, rabbit anti-human antibodies against KLLN (ab221907, 1:500), E-cadherin (ab15148, 1:30), N-cadherin (ab18203, 1:100), Vimentin (ab8978, 1:80), p53 (ab131442, 1:50), Ki67 (ab15580, 1:100), and matrix metalloproteinase-9 (MMP-9) (ab38898, 1:100), for 2 h at 37°C and rinsed with PBS. Following PBS aspiration, the sections were incubated with the secondary antibody, goat anti-rabbit antibody against immunoglobulin G (IgG) labeled with horseradish peroxidase (HRP; ab6721, 1:1,000), at 37°C for 30 min in a wet box. All the aforementioned antibodies were purchased from Abcam (Cambridge, MA, USA).

The sections were then counterstained with hematoxylin (Shanghai Fusheng Industrial, Shanghai, China) at room temperature for 4 min. The section was then mounted with 10% glycerol and PBS and observed under the microscope. The immunohistochemistry results were scored independently by two individuals using the double-blinded method. The experiment was repeated three times.

RIP Assay

The cultured cells were washed twice with cold PBS, added to 10 mL PBS, and transferred into a centrifuge tube. The cells were centrifuged at 1,500 rpm for 5 min at 4°C, after which the supernatant was discarded. The cells were then lysed with 100 mL RIP lysis buffer (N653, Shanghai Haoran Biological Technology, Shanghai, China) on ice for 5 min to obtain the cell lysate. Next, 50 μL magnetic beads was added in each tube, and 0.5 mL RIP wash buffer (EHJ-BVIS08102, Xiamen Huijia Biotechnology, Xiamen, Fujian, China) was added. The beads were washed, re-suspended with 100 μL RIP wash buffer in each tube, followed by the addition of 5 μg argonaute 2 (Ago2) antibody (P10502500, Shenzhen Otwo Biotechnology, Shenzhen, Guangdong, China). The normal mouse antibody to IgG was regarded as the NC, incubated for 30 min at room temperature followed by discarding of the supernatant. The magnetic beads were washed twice with 0.5 mL RIP wash buffer for the subsequent experiment.

Next, 900 μL RIP immunoprecipitation buffer (P10403138, Shenzhen Otwo Biotechnology, Shenzhen, China) was added to the magnetic bead-antibody complexes, after which the cell lysate was centrifuged at 14,000 rpm for 10 min at 4°C. The supernatant was transferred into a new eppendorf (EP) tube (LBCT015S, Beijing North TZ-Biotech Develop, Beijing, China), with 100 μL supernatant transferred into the tube containing magnetic bead-antibody complexes with 1.0 mL as the final volume of the immunoprecipitation reaction. The tubes were subsequently incubated overnight at 4°C, with the magnetic beads washed 6 times with 0.5 mL RIP wash buffer. The RNA was purified with 150 μL proteinase K buffer for 30 min at 55°C. RNA extraction was performed based on the conventional TRIZOL method, followed by detection by means of qRT-PCR.

Western Blot Analysis

The total protein in tissues or cells was extracted by means of radioimmunoprecipitation assay lysis buffer containing phenylmethylsulfonyl (PMSF). The protein was incubated on ice for 30 min at 4°C, and it was centrifuged at 8,000 × *g* for 10 min to collect the supernatant. The total protein concentration was measured using a bicinchoninic acid (BCA) kit. Then, 50 μg protein was dissolved in 2 × SDS loading buffer. After boiling at 100°C for 5 min, the protein was separated by SDS-PAGE. The protein was transferred onto a polyvinylidene fluoride (PVDF) membrane via the wet transfer method, followed by blockade with 5% skim milk powder at room temperature for 1 h. The PVDF membrane was incubated with the primary antibodies, rabbit anti-human antibodies to KLLN (ab197892, 1:500), E-Cadherin (ab15148, 1:500), N-Cadherin (ab76057, 1:1,000), Vimentin (ab92547, 1:2,000), p53 (ab131442, 1:500), and GAPDH (internal reference; ab9485, 1:2,500), overnight at 4°C. The membrane was incubated with the secondary antibody, HRP-labeled

goat anti-rabbit IgG (ab97051, 1:2,000), for 1 h and rinsed with Tris-buffered saline with Tween (TBST). All the aforementioned antibodies were purchased from Abcam (Cambridge, MA, USA).

Solution A and solution B from an enhanced chemiluminescence (ECL) fluorescence detection kit (BB-3501, Amersham Pharmacia Biotech, Piscataway, NJ, USA) were mixed under conditions void of light, followed by dropwise addition onto the membrane, with a gel imager then employed for exposure. The Bio-Rad image analysis system (Bio-Rad, Hercules, CA, USA) was used for image collection, after which Quantity One version (v.)4.6.2 software was utilized for analyses. The relative protein expression was expressed as the gray value of the corresponding protein band to the gray value of the GAPDH protein band. The experiment was repeated three times, and the average value obtained was selected accordingly.

Dual-Luciferase Reporter Gene Assay

The WT and mut reporter plasmids of LINC00472 (WT-LINC00472 and mut-LINC00472) and the WT and mut reporter plasmids of KLLN (WT-KLLN and mut-KLLN) were provided by Shanghai GenePharma (Shanghai, China). The NC mimic, miR-149-3p mimic, and miR-4270 mimic were respectively co-transfected with WT-LINC00472, mut-LINC00472, WT-KLLN, and mut-KLLN into 293T cells. The cells were cultured for 48 h, with the changes in luciferase activity measured based on the instructions of the dual-luciferase reporter gene assay kit (D0010, Beijing Solarbio Technology, Beijing, China). The fluorescence intensity was detected using GLomax 20/20 Luminometer (E5311, Shaanxi Zhongmei Biotechnology, Xi'an, Shaanxi, China). The experiment was repeated three times.

EdU Fluorescence Assay

Cells at the logarithmic growth phase were seeded in the 96-well plates at a density of 5×10^4 cells/well. After adherence to the wells, the cells in each well were incubated for 2 h in 500 μL EdU medium (50 μmoL/L), fixed with 40 g/L paraformaldehyde for 20 min, incubated with 2 mg/mL glycine for 10 min, and washed twice with PBS. Later, the cells were permeabilized with 500 μL 0.5% Triton, and they were permitted to react with Apollo staining solution for 0.5 h under dark conditions, followed by two PBS washes. Afterward, the cells were incubated with Hoechst 33342 reaction solution for 0.5 h under dark conditions, washed twice with 0.5% Triton, and observed under an inverted fluorescence microscope. The professional image analysis software Image-Pro Plus 6.0 was applied to count the cell number.

Transwell Assay

The pre-cooled Matrigel (40111ES08, Shanghai Yeasen Biotechnology, Shanghai, China) diluted with serum-free DMEM at the ratio of 1:8 was used to coat the Transwell apical chamber (3413, Beijing Unique Biotech, Beijing, China) (the step could be ignored in the migration experiment), and it was solidified in a 37°C incubator for 4–5 h. The transfected cells were diluted with 100 μL serum-free medium to prepare a cell suspension at a concentration of about 1×10^6 cells/mL. Later, the cells were inoculated, and 500 μL DMEM containing 20% FBS was added to the basolateral chamber, with 3 replicate wells in each group. The cells were incubated for 24 h at 37°C with 5% CO_2. The transwell chamber was washed twice with PBS, fixed with 5% glutaraldehyde at 4°C, stained with 0.1% crystal violet for 5 min, followed by two additional PBS washes. The cells on the surface were wiped with cotton balls. After that, they were analyzed under an inverted fluorescence microscope (TE2000, Nikon Imaging Sales, Shanghai, China). Five fields were randomly selected for photographing (200×), with the mean value selected as the number of cells passing through the chamber in each group. The experiment was repeated three times.

Tumor Formation in Nude Mice

A total of 12 BALA/c nude mice (without limitation in gender, aged 4 weeks, weighing 18–22 g) was purchased from Guangdong Medical Laboratory Animal Center (Foshan, Guangdong, China) (http://www.gdmlac.com.cn/). The mice were placed in a controlled specific pathogen-free (SPF) environment and randomly divided into two groups (6 mice for each group). The cell lines with stable transfection of oe-NC and oe-LINC00472 were screened and subcutaneously injected into the mice at 1×10^6 NCI-H1299 cells/mouse. The data were recorded on the seventh, 14^{th}, 21^{st}, and 28^{th} days after inoculation. The nude mice were euthanized by means of carbon dioxide asphyxiation following completion of the experiment. The volume calculation formula of the tumor xenograft was as follows: $V\ (mm^3) = (A \times B^2)/2$ where A is the long diameter and B is the short diameter, and the average volume graph at each time point was plotted.

Statistical Analysis

All experimental data statistical analyses were conducted by SPSS 21.0 software (IBM, Armonk, NY, USA). All experiments were repeated three times. Normality and homogeneity of variance were evaluated and confirmed in all the data. Measurement data were expressed as mean ± SD. Paired t test was employed for comparison between the experimental data of NSCLC tissues and adjacent normal tissues. Other comparisons between two groups were analyzed by means of an unpaired t test. Comparisons among multiple groups were analyzed by one-way ANOVA. Pairwise comparison among multiple groups was performed using a post hoc test. Data at different time points were compared by repeated-measure ANOVA. Kaplan-Meier analysis was conducted for survival of NSCLC patients with high or low expression of LINC00472. The correlation of miR-149-3p and miR-4270 with LINC00472 was assessed through Pearson correlation analysis. $p < 0.05$ was considered to be indicative of a statistically significant difference.

SUPPLEMENTAL INFORMATION

Supplemental Information can be found online at https://doi.org/10.1016/j.omtn.2019.06.003.

AUTHOR CONTRIBUTIONS

A.W. and C.Z. designed the study. J.Z., Z.L., and Q.H. collated the data, designed and developed the database, carried out data analyses, and produced the initial draft of the manuscript. A.Z., X.L., and Z.M. contributed to drafting the manuscript. All authors read and approved the final submitted manuscript.

CONFLICTS OF INTEREST

The authors declare no competing interests.

ACKNOWLEDGMENTS

We would like to acknowledge the helpful comments on this paper received from our reviewers.

REFERENCES

1. Liu, Y., Li, M., Zhang, G., and Pang, Z. (2013). MicroRNA-10b overexpression promotes non-small cell lung cancer cell proliferation and invasion. Eur. J. Med. Res. *18*, 41.
2. Wang, Z.X., Bian, H.B., Wang, J.R., Cheng, Z.X., Wang, K.M., and De, W. (2011). Prognostic significance of serum miRNA-21 expression in human non-small cell lung cancer. J. Surg. Oncol. *104*, 847–851.
3. Feng, J., Zhang, X., Zhu, H., Wang, X., Ni, S., and Huang, J. (2012). FoxQ1 overexpression influences poor prognosis in non-small cell lung cancer, associates with the phenomenon of EMT. PLoS ONE *7*, e39937.
4. Ke, Y., Zhao, W., Xiong, J., and Cao, R. (2013). miR-149 Inhibits Non-Small-Cell Lung Cancer Cells EMT by Targeting FOXM1. Biochem. Res. Int. *2013*, 506731.
5. Maeda, R., Yoshida, J., Hishida, T., Aokage, K., Nishimura, M., Nishiwaki, Y., and Nagai, K. (2010). Late recurrence of non-small cell lung cancer more than 5 years after complete resection: incidence and clinical implications in patient follow-up. Chest *138*, 145–150.
6. Xiong, Y., Wang, T., Wang, M., Zhao, J., Li, X., Zhang, Z., Zhou, Y., Liu, J., Jia, L., and Han, Y. (2018). Long non-coding RNAs function as novel predictors and targets of non-small cell lung cancer: a systematic review and meta-analysis. Oncotarget *9*, 11377–11386.
7. Zhan, Y., Zang, H., Feng, J., Lu, J., Chen, L., and Fan, S. (2017). Long non-coding RNAs associated with non-small cell lung cancer. Oncotarget *8*, 69174–69184.
8. Shen, J., Todd, N.W., Zhang, H., Yu, L., Lingxiao, X., Mei, Y., Guarnera, M., Liao, J., Chou, A., Lu, C.L., et al. (2011). Plasma microRNAs as potential biomarkers for non-small-cell lung cancer. Lab. Invest. *91*, 579–587.
9. Yang, L., Wei, H., and Xiao, H.J. (2016). Long non-coding RNA Loc554202 expression as a prognostic factor in patients with colorectal cancer. Eur. Rev. Med. Pharmacol. Sci. *20*, 4243–4247.
10. Wang, L., Zhao, Z., Feng, W., Ye, Z., Dai, W., Zhang, C., Peng, J., and Wu, K. (2016). Long non-coding RNA TUG1 promotes colorectal cancer metastasis via EMT pathway. Oncotarget *7*, 51713–51719.
11. Shen, Y., Wang, Z., Loo, L.W., Ni, Y., Jia, W., Fei, P., Risch, H.A., Katsaros, D., and Yu, H. (2015). LINC00472 expression is regulated by promoter methylation and associated with disease-free survival in patients with grade 2 breast cancer. Breast Cancer Res. Treat. *154*, 473–482.
12. Bellazzo, A., Di Minin, G., Valentino, E., Sicari, D., Torre, D., Marchionni, L., Serpi, F., Stadler, M.B., Taverna, D., Zuccolotto, G., et al. (2018). Cell-autonomous and cell non-autonomous downregulation of tumor suppressor DAB2IP by microRNA-149-3p promotes aggressiveness of cancer cells. Cell Death Differ. *25*, 1224–1238.
13. Tokuhisa, M., Ichikawa, Y., Kosaka, N., Ochiya, T., Yashiro, M., Hirakawa, K., Kosaka, T., Makino, H., Akiyama, H., Kunisaki, C., and Endo, I. (2015). Exosomal miRNAs from Peritoneum Lavage Fluid as Potential Prognostic Biomarkers of Peritoneal Metastasis in Gastric Cancer. PLoS ONE *10*, e0130472.
14. Wang, Y., Radhakrishnan, D., He, X., Peehl, D.M., and Eng, C. (2013). Transcription factor KLLN inhibits tumor growth by AR suppression, induces apoptosis by TP53/TP73 stimulation in prostate carcinomas, and correlates with cellular differentiation. J. Clin. Endocrinol. Metab. *98*, E586–E594.
15. Zhong, G., Chen, X., Fang, X., Wang, D., Xie, M., and Chen, Q. (2016). Fra-1 is upregulated in lung cancer tissues and inhibits the apoptosis of lung cancer cells by the P53 signaling pathway. Oncol. Rep. *35*, 447–453.
16. Wang, Y., He, X., Yu, Q., and Eng, C. (2013). Androgen receptor-induced tumor suppressor, KLLN, inhibits breast cancer growth and transcriptionally activates p53/p73-mediated apoptosis in breast carcinomas. Hum. Mol. Genet. *22*, 2263–2272.
17. Silwal-Pandit, L., Vollan, H.K., Chin, S.F., Rueda, O.M., McKinney, S., Osako, T., Quigley, D.A., Kristensen, V.N., Aparicio, S., Børresen-Dale, A.L., et al. (2014). TP53 mutation spectrum in breast cancer is subtype specific and has distinct prognostic relevance. Clin. Cancer Res. *20*, 3569–3580.
18. Haricharan, S., and Brown, P. (2015). TLR4 has a TP53-dependent dual role in regulating breast cancer cell growth. Proc. Natl. Acad. Sci. USA *112*, E3216–E3225.
19. Li, X.L., Zhou, J., Chen, Z.R., and Chng, W.J. (2015). P53 mutations in colorectal cancer - molecular pathogenesis and pharmacological reactivation. World J. Gastroenterol. *21*, 84–93.
20. Mishra, A., Brat, D.J., and Verma, M. (2015). P53 tumor suppression network in cancer epigenetics. Methods Mol. Biol. *1238*, 597–605.
21. Acunzo, M., Visone, R., Romano, G., Veronese, A., Lovat, F., Palmieri, D., Bottoni, A., Garofalo, M., Gasparini, P., Condorelli, G., et al. (2012). miR-130a targets MET and induces TRAIL-sensitivity in NSCLC by downregulating miR-221 and 222. Oncogene *31*, 634–642.
22. Shen, Y., Katsaros, D., Loo, L.W.M., Hernandez, B.Y., Chong, C., Canuto, E.M., Biglia, N., Lu, L., Risch, H., Chu, W.M., and Yu, H. (2015). Prognostic and predictive values of long non-coding RNA LINC00472 in breast cancer. Oncotarget *6*, 8579–8592.
23. Fu, Y., Biglia, N., Wang, Z., Shen, Y., Risch, H.A., Lu, L., Canuto, E.M., Jia, W., Katsaros, D., and Yu, H. (2016). Long non-coding RNAs, ASAP1-IT1, FAM215A, and LINC00472, in epithelial ovarian cancer. Gynecol. Oncol. *143*, 642–649.
24. Ye, Y., Yang, S., Han, Y., Sun, J., Xv, L., Wu, L., Wang, Y., and Ming, L. (2018). Linc00472 suppresses proliferation and promotes apoptosis through elevating PDCD4 expression by sponging miR-196a in colorectal cancer. Aging (Albany N.Y.) *10*, 1523–1533.
25. Zhu, T.G., Xiao, X., Wei, Q., Yue, M., and Zhang, L.X. (2017). Revealing potential long non-coding RNA biomarkers in lung adenocarcinoma using long non-coding RNA-mediated competitive endogenous RNA network. Braz. J. Med. Biol. Res. *50*, e6297.
26. Castellano, J.J., Navarro, A., Viñolas, N., Marrades, R.M., Moises, J., Cordeiro, A., Saco, A., Muñoz, C., Fuster, D., Molins, L., et al. (2016). LincRNA-p21 impacts prognosis in resected non-small cell lung cancer patients through angiogenesis regulation. J. Thorac. Oncol. *11*, 2173–2182.
27. Xie, X., Liu, H.T., Mei, J., Ding, F.B., Xiao, H.B., Hu, F.Q., Hu, R., and Wang, M.S. (2014). LncRNA HMlincRNA717 is down-regulated in non-small cell lung cancer and associated with poor prognosis. Int J Clin Exp Pathol *7*, 8881–8886.
28. Ge, Q.M., Huang, C.M., Zhu, X.Y., Bian, F., and Pan, S.M. (2017). Differentially expressed miRNAs in sepsis-induced acute kidney injury target oxidative stress and mitochondrial dysfunction pathways. PLoS ONE *12*, e0173292.
29. Zuo, B., Zhai, J., You, L., Zhao, Y., Yang, J., Weng, Z., Dai, L., Wu, Q., Ruan, C., and He, Y. (2017). Plasma microRNAs characterising patients with immune thrombocytopenic purpura. Thromb. Haemost. *117*, 1420–1431.
30. Hamam, R., Ali, A.M., Alsaleh, K.A., Kassem, M., Alfayez, M., Aldahmash, A., and Alajez, N.M. (2016). microRNA expression profiling on individual breast cancer patients identifies novel panel of circulating microRNA for early detection. Sci. Rep. *6*, 25997.
31. Hu, K., and Liang, M. (2017). Upregulated microRNA-224 promotes ovarian cancer cell proliferation by targeting KLLN. In Vitro Cell. Dev. Biol. Anim. *53*, 149–156.
32. Wei, G.H., and Wang, X. (2017). lncRNA MEG3 inhibit proliferation and metastasis of gastric cancer via p53 signaling pathway. Eur. Rev. Med. Pharmacol. Sci. *21*, 3850–3856.
33. Su, C., Shi, K., Cheng, X., Han, Y., Li, Y., Yu, D., and Liu, Z. (2018). Long Noncoding RNA LINC00472 Inhibits Proliferation and Promotes Apoptosis of Lung Adenocarcinoma Cells via Regulating miR-24-3p/ DEDD. Technol. Cancer Res. Treat. *17*, 1533033818790490.
34. Hao, Y., Yang, X., Zhang, D., Luo, J., and Chen, R. (2017). Long noncoding RNA LINC01186, regulated by TGF-β/SMAD3, inhibits migration and invasion through Epithelial-Mesenchymal-Transition in lung cancer. Gene *608*, 1–12.
35. Kong, J., Sun, W., Li, C., Wan, L., Wang, S., Wu, Y., Xu, E., Zhang, H., and Lai, M. (2016). Long non-coding RNA LINC01133 inhibits epithelial-mesenchymal transition and metastasis in colorectal cancer by interacting with SRSF6. Cancer Lett. *380*, 476–484.

OMTN, Volume *17*

Supplemental Information

LINC00472 Acts as a Tumor Suppressor in NSCLC through KLLN-Mediated p53-Signaling Pathway via MicroRNA-149-3p and MicroRNA-4270

Aimei Zou, Xingli Liu, Zongjiong Mai, Junke Zhang, Zhuohuan Liu, Qilu Huang, Aibing Wu, and Chenyu Zhou

Supplementary Table 1 Differential expression of the top 15 significantly up-regulated microRNAs in the GSE53882 chip

Name	logFC	AveExpr	t	*p*.Value	adj.*p*.Val	B
hsa-miR-4459	9.598201879	52.41809664	4.590563763	5.49E-06	2.73E-05	3.297152353
hsa-miR-4270	9.495364803	50.69225472	4.007088624	7.00E-05	0.00025993	0.888602066
hsa-miR-4728-5p	6.90720549	21.46348703	7.460990394	3.40E-13	9.48E-12	19.34353027
hsa-miR-1469	6.542374927	26.86103262	6.369190659	4.03E-10	4.64E-09	12.45681221
hsa-miR-4741	6.316713619	27.20804924	4.620814198	4.77E-06	2.42E-05	3.430307931
hsa-miR-197-5p	5.735529116	69.13321789	2.407625564	0.016386847	0.03320635	-4.105704295
hsa-miR-4634	5.344022902	15.21173948	7.244535933	1.48E-12	3.14E-11	17.90639843
hsa-miR-4651	4.861107788	16.3845797	7.409265705	4.85E-13	1.28E-11	18.99696503
hsa-miR-1273g-3p	4.570442955	17.77522159	3.581701057	0.000371803	0.001151027	-0.672804786
hsa-miR-4298	4.320193041	16.10696669	7.325308268	8.60E-13	1.98E-11	18.43862771
hsa-miR-3937	3.515555541	9.259725287	7.387755993	5.62E-13	1.42E-11	18.85342479
hsa-miR-4497	3.311147292	23.03851373	5.156352264	3.53E-07	2.28E-06	5.920238497
hsa-miR-4667-5p	3.14648062	21.53320027	4.036624426	6.20E-05	0.000231993	1.003156522
hsa-miR-149-3p	3.051866257	28.54811444	2.827980094	0.004856015	0.011394623	-3.026579112
hsa-miR-1268a	3.003126289	13.90278803	6.142301797	1.57E-09	1.63E-08	11.14219008